Precision Agric (2014) 15:479–498
DOI 10.1007/s11119-014-9347-8

An approach for assessing the effects of site-specific fertilization on crop growth and yield of durum wheat in organic agriculture

M. Diacono · A. Castrignanò · C. Vitti · A. M. Stellacci · L. Marino · C. Cocozza · D. De Benedetto · A. Troccoli · P. Rubino · D. Ventrella

Published online: 1 February 2014

Abstract Precision agriculture (PA) technologies allow us to assess field variability and support site-specific (SSP) application of inputs. The joint application of PA and organic farming practices might be synergetic. The objective of this 3-year study was to propose a multivariate statistical and geostatistical approach, to evaluate the effects of SSP nitrogen (N) fertilization on durum wheat in transition to organic farming. Soil parameters were measured to assess soil fertility level before the SSP fertilization on wheat, which was carried out by management zones in the third year. Radiometric measurements were performed with a hyperspectral spectroradiometer and N-uptake at anthesis and grain yield were determined. The expected values and 95 % confidence intervals of the soil parameters, N-uptake and yield data were estimated with polygon kriging for each management zone. Reflectance data were reduced through principal component analysis and the retained principal components were submitted to factorial co-kriging analysis to estimate orthogonal scale-dependent factors. Comparisons between N-uptake and yield and between the retained regionalized factors (F1) and yield were performed. The spatial pattern of F1 at shorter scales was mostly reproduced in the N-uptake map, suggesting the predictive capacity of hyperspectral data for crop N-status. Within-cluster variance for yield was reduced, quite probably as a combined effect of meteorological pattern and management.

M. Diacono (✉) · P. Rubino
Dipartimento di Scienze Agro-ambientali e Territoriali, University of Bari, Via Amendola 165/a, 70126 Bari, Italy
e-mail: mariangela.diacono@inwind.it

M. Diacono · A. Castrignanò · C. Vitti · A. M. Stellacci · D. De Benedetto · D. Ventrella
Consiglio per la ricerca e la sperimentazione in agricoltura - Unità di ricerca per i sistemi colturali degli ambienti caldo-aridi (Bari), Via C. Ulpiani 5, 70125 Bari, Italy

L. Marino · C. Cocozza
Dipartimento di Scienze del Suolo, della Pianta e degli Alimenti, University of Bari, Via Amendola 165/a, 70126 Bari, Italy

A. Troccoli
Consiglio per la ricerca e la sperimentazione in agricoltura - Centro di ricerca per la cerealicoltura, S.S. 16, km 675, 71122 Foggia, Italy

The preliminary results seem to be promising in the perspective of PA. Moreover, an inverse relationship between grain yield and crop N-status was observed.

Keywords Precision fertilization · Hyperspectral data · Plant response · Grain yield variability · Polygon kriging

Introduction

Sustainability refers to agricultural practices technically appropriate, economically and environmentally viable that meet society needs for food, feed, ecosystem services and human health for present and future generations (FAO 1995). Crop rotations including leguminous crops, organic fertilizers and soil amendments (e.g., composts) can increase or preserve soil organic matter content that plays an important role in sustaining overall soil fertility. These practices are the main tools in the organic farming management that avoids the use of synthetic fertilizers and pesticides (Maeder et al. 2002). However, conversion to organic farming frequently comes along with a decline in crop yields, whereas the growth of world population would require an intensification of production while reducing environmental impact (Mueller et al. 2012).

Nitrogen (N) is the largest agricultural input used by wheat farmers but its overuse causes environmental concerns (Shepherd et al. 1993). Despite fields differ spatially in crop requirements, they are mostly managed as homogenous units, often locally receiving an excessive rate of N. Conversely, precision agriculture (PA) takes into account spatial and temporal variability of soil and canopy properties, supporting site-specific (SSP) application of inputs. Therefore, the joint application of PA management technologies and organic farming practices might be synergetic, sustaining soil fertility and food production by reducing the impact of agricultural activity and preserving the environmental resources.

Several studies have demonstrated the advantages of SSP fertilization practices in cereal crop systems (Li et al. 2009; Tubaña et al. 2008) even if no one, as far as we know, has focused on such PA practices applied in transition to organic farming. Delineating management classes may form the basis for spatially variable application of inputs (e.g., fertilizers), once the factors responsible for yield variability have been identified. Polygon (co)kriging can be used to give the expected value and (co)kriging standard deviation of the variables, for each management zone since, differently to traditional averaging, takes spatial dependence into account. Diacono et al. (2012) have confirmed the important role of climatic conditions in altering the spatial distribution of rainfed crop response. Therefore, it is worthwhile to monitor cereal crops during their growth, for timely detecting the spatial variability of plant response to nutrients availability. Spectral measurements of wheat canopy, collected with hyperspectral proximal sensors, have proved to be quite promising to indirectly detect crop N-status, during crop growth, at a very high spatial resolution (Li et al. 2010). The numerous narrow, contiguous spectral bands can be exploited to identify regions of the spectrum that are more sensitive to plant N-status (Stroppiana et al. 2009). In particular, multivariate statistical techniques, such as principal component analysis (PCA), can play a critical role for dimensionality reduction aiming at deriving a new set of orthogonal factors explaining the pattern of correlations and capturing most variance of the original hyperspectral data (Ray et al. 2010). Yield monitoring by combine harvesters could be afterwards used to validate sensor-based predictive technology of spatial variability of wheat production (Prasad et al. 2007).

The novelty of the present work is to test and propose a new statistical approach, based on multivariate geostatistics, and particularly polygon (co)kriging, aimed at multiple comparisons of durum wheat response, among different clusters, taking into account the spatial correlation observed in the field. The joint application of PA management technologies and organic farming practices might innovate organic farming.

Materials and methods

Site of study and experimental setup

The research was carried out at the experimental farm of Cereal Research Centre, located in Foggia (southern Italy, 41°27′36.720″N, 15°30′03.494″E; 90 m a.s.l.), during the 2009–2010, 2010–2011 and 2011–2012 crop seasons. The study was conducted on a 2-year "wheat (*Triticum durum* Desf. cv Claudio)-chickpea (*Cicer arietinum* L. cv Sultano)" rotation, in a 3-ha field under organic farming management. In the third year the research was carried out on wheat crop and results were compared with those of the first season.

The field is located in a flat area called "Apulian Tavoliere" and the soil is of alluvial origin classified as Typic Calcixerept (Soil Survey Staff 1999). The area is characterized by climatic conditions of a typical Mediterranean environment.

The climatic data used, i.e., daily minimum and maximum air temperature and cumulative precipitation, were recorded at the agro-meteorological station of the neighboring experimental farm "Podere 124" (Foggia, 41°26′49″N, 15°30′15″E, 90 m a.s.l.).

Soil sampling and measurements

The first soil sampling was carried out at the beginning of the crop rotation (in November 2009). Samples (0.30-m depth) were collected from 50 georeferenced locations evenly distributed on the field. Moreover, in July 2011, after the chickpea crop, soil samples were collected at the same locations. This sampling was carried out to compare the soil fertility level before the second cultivation of wheat with that characterizing the initial conditions. The number of samples was sufficient for variogram estimation according to Webster and Oliver (2001), who recommend collection of at least 50 sampling points.

The soil samples were air dried, ground to pass a 2-mm sieve and then analyzed for the following parameters determining soil fertility: nitrogen content (N; g kg^{-1}) by the Kjeldahl method; available phosphorus (P_{av}; mg kg^{-1}) according to Olsen and Sommers (Page et al. 1982) by using the ammonium molybdate-ascorbic acid method; exchangeable potassium (K_{ex}; mg kg^{-1}) extracted by $BaCl_2$ and $N(CH_2OHCH_2)_3$, according to Page et al. (1982) methodologies, and assayed by inductively coupled plasma-optical emission spectrometry (ICP-OES); total organic carbon (TOC; g kg^{-1}) determined by using the Walkley–Black method (Walkley and Black 1934).

Agronomic management

The field was previously divided into four management zones (Fig. 1), by using soil data collected at the beginning of the trial (November 2009). A combined approach of geostatistics and non-parametric density function algorithm of clustering was applied to a multivariate data set including soil carbon (C) loss by mineralization and main physical–chemical

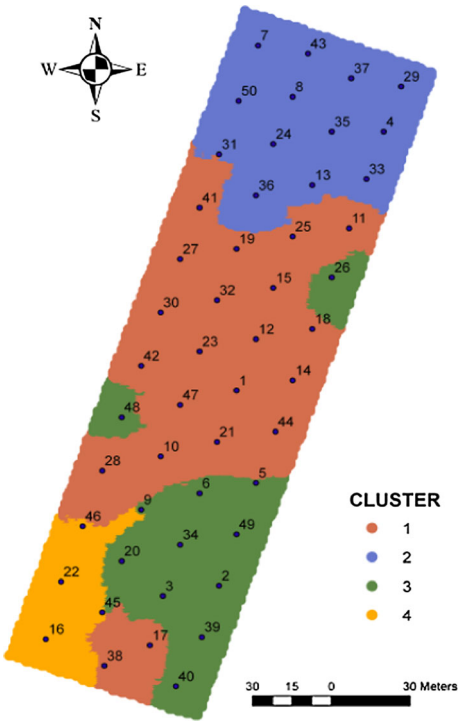

Fig. 1 Homogeneous sub-field zones, as delineated in Diacono et al. (2011), and georeferenced sampling points

soil variables (clay content, N, P_{av}, K_{ex}, TOC and pH). More details can be found in Diacono et al. (2011). Since C loss negatively affects soil fertility, on the basis of the average C mineralization rate (defined as grams of C mineralized per kilogram of TOC of soil) the northern zone of the field (cluster 2, Fig. 1) with 0.15 g C mineralized kg^{-1} TOC and the highest clay content, might potentially conserve more C in the long-term period, and might then be considered as the most fertile, while cluster 3 corresponded to the relatively less fertile area (0.18 g C mineralized kg^{-1} TOC; lowest clay content). Finally, clusters 1 and 4 were merged, since their TOC content (11.2 g kg^{-1}) and loss values (0.16 g C mineralized kg^{-1} TOC) were quite similar, and could be classified as a medium soil fertility zone (subsequently called cluster 1).

The borders of the resultant three clusters were rectified by drawing 10 × 330-m strips, parallel to the longer axis of the field, in order to facilitate the work of the spreader. Cluster 2 was assumed as a reference and fertilized according to the local good agricultural practices (about 45 kg P_2O_5 ha^{-1} for chickpea, and 100 kg N ha^{-1} for wheat in the third year). In each of the other clusters, the increment of organic fertilizer was calculated by multiplying the reference rate by the ratio of the C mineralized in a cluster to that of the "reference" cluster.

Therefore, in the second-year trial (January 2011), an organic P fertilizer (Guanito, Italpollina spa, characterized by 15 % P_2O_5, 55 % organic matter; allowed in organic farming) was applied on chickpea, as follows: 49.5 kg P_2O_5 ha^{-1} in cluster 1; 45 kg P_2O_5 ha^{-1} in cluster 2; 54 kg P_2O_5 ha^{-1} in cluster 3. Unfortunately, leguminous and non-leguminous weeds emerged in the winter-sown chickpea crop creating heavy competition, despite several mechanical operations of weeds control were applied.

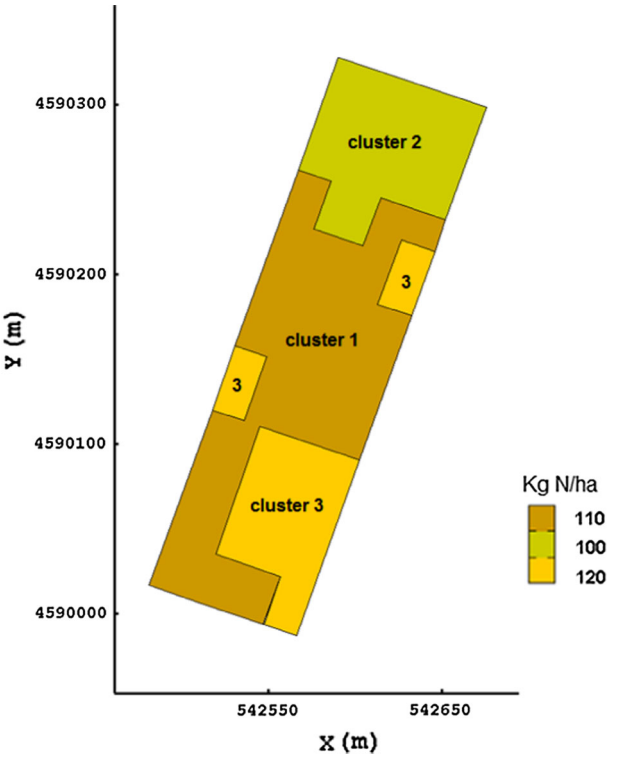

Fig. 2 Fertilizer rates (kg N ha^{-1}) applied site-specifically in each homogeneous area

For this reason, in late spring 2011 the whole green biomass (weeds and chickpea plants) was cut up and incorporated into the soil up to 35–40 cm of depth as "green manure". The field site was then tilled, in late summer, by plowing and disk harrowing to prepare seedbed.

A commercial organic N fertilizer (Fertil, ILSA, characterized by: 12.5 % organic N, 70 % organic matter; allowed in organic farming) was applied on wheat in early December 2011. Fertil has a high N content because it is obtained from collagen by a standardized thermal hydrolysis process. This process produces a slow-release N product named AGROGEL® that is characterized by 95 % of extractable organic C and low C/N rate. Contrary to the first-year trial, when a uniform fertilization rate of about 80 kg N ha^{-1} was applied in December 2009, fertilization was carried out site-specifically by the homogeneous zones previously determined, following the criteria described above. Therefore, the fertilizer was applied to supply the following N rates: 110 kg N ha^{-1} to cluster 1, 100 kg N ha^{-1} to cluster 2 and 120 kg N ha^{-1} to cluster 3 (Fig. 2). Each SSP fertilization was carried out in one stage (before sowing) by using an AMAZONE PROFIS ZA-M 1500 centrifugal broadcaster (AMAZONEN-WERKE H. DREYER GmbH & Co. KG, Germany). The fertilizer was incorporated with a disc harrow to 15-cm depth and sowing was done in mid-December 2011, at a rate of 350 seeds m^{-2} and with a between-row space of 17 cm.

Finally, the wheat straw and stubble were buried in 2010 and 2012, according to the soil fertility management in organic agriculture.

Spectral reflectance measurements

Reflectance data were gathered in two stages of crop growth of the last trial year: in March 2012, at stem elongation (growth stage, GS 30, Zadoks et al. 1974) and in April 2012, at beginning of anthesis (GS 60).

The ASD FieldSpec® HandHeld (ASD Inc., Boulder, CO, USA) was used (Li et al. 2010), which is a high resolution hyperspectral radiometer covering the wavelengths from 325 to 1 075 nm. The instrument, which relies on a 512-element photodiode array, acquires hyperspectral data with a spectral resolution (full width at half maximum) of 3.5 nm at around 700 nm and a sampling interval of 1.5 nm (spacing between sample points in the measured spectrum). The field of view (FOV) of the bare fiber-optic probe is 25°. The reflectance of the target was calculated with the calibration measurements of dark current and a white reference panel with known reflectance properties.

The sensor was held approximately 50 cm above the canopy in nadir orientation, producing a spot of approximately 250-cm^2 size deemed sufficient to reduce the soil background effects. To minimize operator influence, the radiometer was mounted on a tripod boom and the same operator made each reading. At each stage 100 spectral measurements (two readings per each of the 50 locations) were made under clear and cloudless sky conditions between 11:00 a.m. and 2:00 p.m. at local time, to provide the best conditions for passive recording.

Biomass and N measurements

Only at GS 60 aboveground biomass was also collected over areas of 0.17 m^2 (1 m × 0.17 m) in proximity of the 50 sampling locations, where the spectral readings had been previously carried out. The fresh biomass was put into plastic bags, immediately weighed and, after oven-drying at 70 °C till to constant weight, dry biomass of each sample was quantified. The GS 60 was chosen as one of the most informative phenological stages (Prasad et al. 2007), relating to efficiency of N-uptake and transfer to grain. Plant samples were milled and total N content (g N g^{-1} dry weight) was detected with a CHNS elemental analyzer (Flash EA 1112, Thermo Scientific) (Horneck and Miller 1998). Aboveground N-uptake was calculated as the product: aboveground biomass dry weight × total N content.

Yield monitoring

At harvesting (on June 25th 2012), yield data were recorded with a John Deere combine (model 9660i WTS) equipped with a yield monitor system (grain mass flow and moisture sensors) (GREENSTAR Yield Monitor System and Yield Mapping System—DEERE & COMPANY, Moline, IL, USA). The data were recorded using a block size of about 2 m along the driving direction and 6 m on the orthogonal direction. After recording, yield data were firstly normalized to 13 % moisture content of grain and then cleaned, by removing the values less than 1.6 t ha^{-1} and greater than 7 t ha^{-1}, according to an evaluation of the minimum and the maximum yields obtainable in the study area, and the outliers differing more than 3 standard deviations from the field average. The same procedures had been also used in the first year of the trial (2010).

Data analysis

Geostatistical and statistical procedures

Variogram modelling is sensitive to strong departures from normality, because a few exceptionally large outliers may contribute to very large squared differences (Wackernagel 2003). To avoid this problem, Gaussian approach was used which consists of different steps, starting with transformation of the initial attributes into Gaussian-shaped variables with zero mean and unit variance. This procedure, known as 'Gaussian anamorphosis', consists of determining a mathematical function to transform standardized Gaussian variable into a variable with any distribution. This transformation is made by using an expansion of Hermite polynomials restricted to a finite number (not greater than 100) of terms (Wackernagel 2003). Preliminarily to interpolation of a multivariate data set, modelling of spatial dependence functions between the variables is required by using the so-called linear model of co-regionalization (LMC). LMC fitting was performed by weighted least-squares technique under the constraint of positive semi-definiteness of the scale-dependent matrix of sills (co-regionalization matrix) (Castrignanò et al. 2000), through an iterative procedure (Lajaunie and Béhaxétéguy 1989). Co-kriging was then applied to estimate the variables at the nodes of a 1 × 1 m-cell grid and the co-kriged estimates were then submitted to back transformation, through the mathematical model calculated in the Gaussian anamorphosis.

Further the 95 % upper and lower limits of confidence interval (CI) of the Gaussian estimates were calculated and they were then back transformed through the Gaussian anamorphosis to calculate the 95 % CIs of the raw variables.

To estimate few scale-dependent regionalized factors summarizing most spatial variance of data, Factorial co-kriging analysis (FKA) was applied (Matheron 1982), consisting in the following steps: (i) fitting a LMC; (ii) analyzing the correlation structure of variables by applying PCA on each co-regionalization matrix, so that a set of orthogonal components, the scale-dependent regionalized factors, can be extracted; (iii) co-kriging and mapping the regionalized factors.

We tested the goodness of fitting by using cross-validation, calculating two statistics: mean error and mean squared standardized error, whose optimal values should be zero and one, respectively (Wackernagel 2003).

Polygon (co)kriging procedure was used to provide the expected value and standard deviation of the variables for each cluster (polygon) of the field delineation. Polygon (co)kriging technique is an extension of block (co)kriging using a special neighborhood definition. It estimates the expected value of a variable over an irregular shape (i.e., a polygon) and the standard deviation of estimation. The polygon is first discretized in regular cells v_i by the user. The procedure is then similar to that of block kriging, except for the calculation of the average co-variance function ($K_{\alpha v}$) for each polygon v, which is calculated as a weighted discrete summation:

$$K_{\alpha v} = \frac{1}{\sum_i w_i} \sum_{i=1}^{N} w_i K_{\alpha c_i}$$

where each w_i corresponds to the surface of the intersection between the cell v_i centered in the point c_i and the polygon v, α is a data point, and $K_{\alpha ci}$ is the covariance function calculated at each point c_i.

The geostatistical analyses were performed by using the software package ISATIS®, release 12.4 (Geovariances 2012).

Soil and yield data analysis

The 2009 soil data set was submitted to a multivariate approach, because of the significant ($p < 0.05$) correlations among the variables. Data were interpolated by using polygon co-kriging procedure.

The 2011 soil data set was split into two subgroups, on the basis of correlation coefficient: (i) the first subset included C for which a univariate approach was used, because it did not show significant correlation ($p > 0.05$) with the other variables, and it was interpolated by polygon kriging; (ii) the second subset included N, P_{av} and K_{ex} for which a multivariate approach was preferred, because of the significant ($p < 0.05$) correlations among the variables: they were interpolated by polygon co-kriging.

The yield-monitored data of each (2009–2010 and 2011–2012) wheat crop season were submitted to univariate analysis, consisting in variogram fitting and interpolation by point kriging to produce a continuous map and polygon kriging for cluster map.

The 95 % upper and 95 % lower limits of CI were also calculated for soil and yield data.

Reflectance and N uptake data analysis

Reflectance data collected at the two growth stages (GS 30 and 60) were firstly aggregated into eight bands [1. Coastal (400–450 nm); 2. Blue (450–510 nm); 3. Green (510–580 nm); 4. Yellow band (585–625 nm); 5. Red (630–690 nm); 6. Red-edge (705–745 nm); 7. and 8. Near-infrared (NIR1 and NIR2) bands (770–895 nm and 860–1 040 nm, respectively)], of the electromagnetic spectrum chosen on the basis of their capabilities to highlight specific vegetation features (Digital Globe 2009).

Previous studies have shown that neighboring wavebands can frequently provide similar information, hence becoming redundant (Thenkabail et al. 2004). A multivariate approach was then used to reduce wavelengths within the eight intervals to few new components describing the multi-frequency variation (Stellacci et al. 2012). PCA was performed, separately for each spectral interval, on the reflectance data previously standardized to mean zero and variance 1 and only the principal components (PCs) with eigenvalue greater than 1 (Kaiser criterion; Kaiser 1960) were retained for further analysis. The component loadings were used to interpret the meaning of the new variables. The PCA approach was implemented by using the FACTOR procedure of SAS/STAT software package (SAS® 9.3 2012). Then, the retained PCs were submitted to FKA, in order to summarize the spatial variance of hyperspectral data into few scale-dependent regionalized factors, and the FKA analysis was repeated for each date of measurements. Subsequently, N-uptake and the selected PCs, which were significantly correlated ($p < 0.05$) with it, were jointly submitted to co-kriging analysis to produce the continuous map of N-uptake. Polygon kriging was also used to provide the expected value, the 95 % upper and 95 % lower limits of CI of the N-uptake for each cluster.

Relationship between crop growth response and wheat yield after site-specific fertilization

Comparisons between N-uptake and yield, as well as between the retained regionalized factors for hyperspectral data and yield, in 2012, were quantitatively performed through two-way contingency matrices, where in each cell there were reported frequency, overall percentage, percentage per row and percentage per column. The overall accuracy, which is a measure of spatial agreement between the two types of maps, was also computed as the proportion of the trace of the contingency matrix. Bowker's test of symmetry (Bowker 1948) was computed, to test the null hypothesis that the percentages are symmetric for all pairs of cells, which implies marginal homogeneity. Weighted kappa coefficient (k) introduced by Cohen (1960) was also used. In addition to the coefficient, its confidence limits were calculated. The approach was implemented with the FREQ procedure of the SAS/STAT software package (SAS® 9.3 2012).

Results and discussion

Weather conditions

In Fig. 3 the monthly mean temperatures and the rainfall for 2009–2010 and 2011–2012 wheat cropping seasons were compared with the long-term averages (1951–2007).

The cumulative rainfall from November to July was higher in 2009–2010 (525 mm) than in 2011–2012 (308 mm) and the latter was lower than the long-term 56-year average (422 mm). The wheat vegetative cycle in the trial area generally occurs from December to

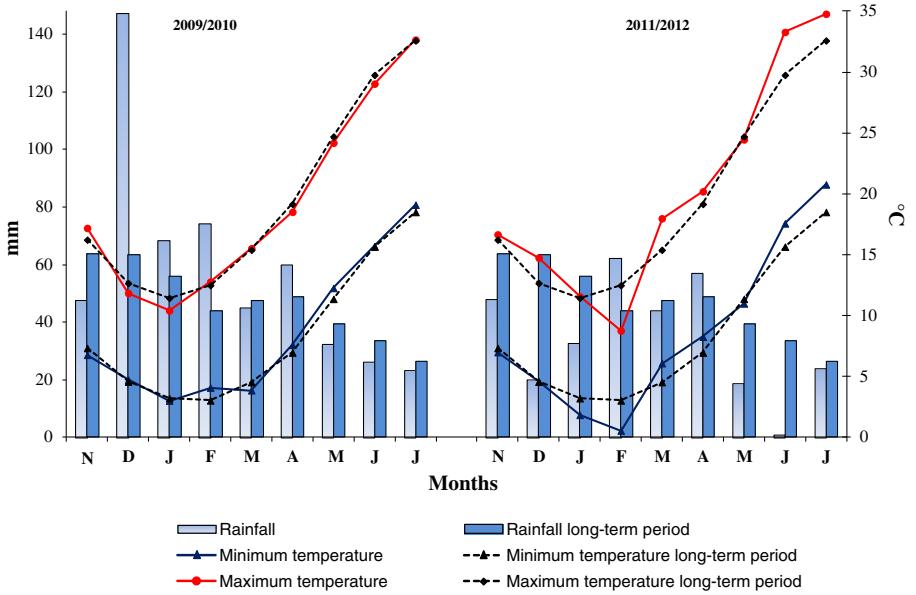

Fig. 3 Mean monthly temperature and rainfall at the study site in each wheat growing season (2009–2010 and 2011–2012), compared with long-term values (1951–2007)

March, while the reproductive period in April–June. In this study, about 335, 160 and 210 mm of rainfall fell during the vegetative cycle in the 2009–2010, 2011–2012 seasons and on the long-term mean, respectively.

The average minimum temperatures of the wheat growing seasons were slightly higher than the long-term mean. The averaged maximum temperature was higher in 2011–2012 by 9 and 6 %, compared to that of 2009–2010 and to the mean of the 56-year period, respectively, during the critical phase of grain maturation (April–June). The 2011–2012 wheat cropping season was then drier and warmer than the 2009–2010 season.

Soil fertility comparison at two stages of crop rotation

Soil parameter values at the two sampling dates (2009 and 2011) were compared for each cluster, to test the variation of soil fertility level at the end of the first 2 years of the trial, after organic fertilization.

K_{ex} (Fig. 4a) and P_{av} (Fig. 4b) revealed a significant decrease over time, probably because of (i) the higher uptake of these nutrients during the rotation, in comparison to the fertilizers and crop residues inputs, and/or (ii) their immobilization into plant debris still undecomposed, since the green manuring in 2011 occurred few weeks before the soil sampling, and/or (iii) retrogradation of P.

The TOC (Fig. 4c) did not show any statistically significant difference probably due to the change of soil management (use of organic fertilizer and green manure, recycle of crop residues) that tends to keep and possibly to increase the soil C content. The slight tendency to lower TOC content in 2011 is probably related to the different sampling time: in fact, the

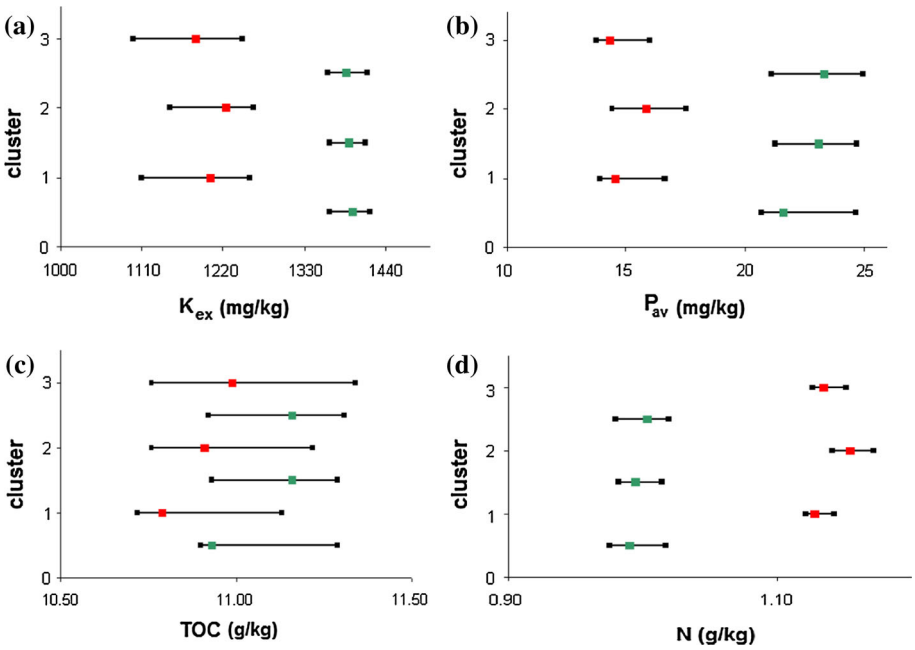

Fig. 4 95 % lower limit, expected value (*green* and *red* for the 2009 and 2011 results, respectively), 95 % upper limit of CI for exchangeable potassium (**a**), available phosphorus (**b**), TOC (**c**) and nitrogen (**d**) (Color figure online)

2009 TOC content was referred to a more preservative period (winter), while the 2011 soil samples were collected in summer. On the other hand, N (Fig. 4d) showed higher values in 2011 than in 2009, because of the N fixation of chickpea, although choked with weeds, and the following green manuring. However, the 2-year trial period could be not sufficient to draw general conclusions on these findings and longer-period experimental data are needed.

Effects of site-specific fertilization on wheat crop growth

Hyperspectral plant response

Only the first principal component (PC1) was retained for each spectral interval (except for Red-edge), explaining more than 95 % of the total variance (Table 1). The results confirmed the high correlation existing between neighboring wavelengths and underlined the importance of adopting multivariate statistical techniques in order to reduce data dimensionality and synthesize redundant information.

In the case of Red-edge band, also the second principal component (PC2) was retained because it showed eigenvalue greater than 1 and explained about 18 % of total Red-edge band variance (Table 1). PC1_Red-edge was mainly correlated to the wavelengths of the 721–728 range, whereas PC2_Red-edge was characterized by greater positive loadings in the 705–710 interval. The existence of two significant components in the Red-edge interval can be attributed to the wide variability of plant radiometric response in this spectral region. This is probably related to the nature of the Red-edge which is a transition spectral region (on the S-shaped reflectance curve) between Red absorption and NIR reflectance (Barnes et al. 2000).

A LMC was then fitted to the experimental direct and cross-variograms of the retained PCs data set, including, as basic structures, a nugget effect and two spherical models with ranges of 60 m and 140 m in March, and 80 and 140 m in April. The goodness of fitting was generally satisfactory, because the mean error was varying between −0.0073 and 0.0228, in March; and between −0.0093 and 0.0065, in April; whereas the mean squared standardized error was between 0.8294 and 1.2312 in March; and between 0.8534 and 1.1546, in April, within the tolerance of ±0.42 from 1 (Chilès and Delfiner 1999).

As the sum of the eigenvalues at each spatial scale gives an estimate of the variance at that scale, the contribution of the longer range component to the total variance was the least in any case. The spatial component of variation at the shorter scale accounted for 48 and 20 % of the total variation in March and April, respectively, whereas the longer scale component accounted for 19 and 15 % of the total variation in March and April, respectively. Therefore, most radiometric variation occurred at the shorter scales, which should be taken into account in strategic decision-making for inputs management. We then retained only the regionalized factor (F1) at the shorter scale at both dates, whereas the nugget effect and longer range factors were omitted, because the former was mainly related to variation at distances less than sampling scale and to experimental error, and the latter explained only a small percentage of the total variance.

In March about 94 % of the variation at short range (60-m scale) was explained by F1 (Table 2), on which PC1_Coastal, PC1_Blue, PC1_Yellow and PC1_Red, mostly related to light absorption by chlorophyll, weighed mainly and negatively.

In April, F1 explained approximately 96 % of variance at 80-m scale and was mostly and negatively affected by the PC1_Green and PC1_Red-edge. Reflectance in these band intervals is able to discriminate plants of different vigor and health. These results underline

Table 1 Eigenvalue and percentage of variance explained by the first two principal components (PCs) of each examined spectral interval, for the two sampling dates, March (a) and April (b)

Spectral band	Range (nm)	No. of variables	PCs	Eigenvalue	% of variance explained
a)					
Coastal	400–450	51	PC1_Coastal	50.63	99.28
			PC2_Coastal	0.18	0.36
Blue	450–510	61	PC1_Blue	60.90	99.84
			PC2_Blue	0.05	0.09
Green	510–580	71	PC1_Green	69.24	97.53
			PC2_Green	1.68	2.37
Yellow	585–625	41	PC1_Yellow	40.83	99.60
			PC2_Yellow	0.12	0.30
Red	630–690	61	PC1_Red	60.77	99.64
			PC2_Red	0.17	0.29
Red-edge	705–745	41	PC1_Red-edge	33.53	81.76
			PC2_Red-edge	7.41	18.09
NIR1	770–895	126	PC1_NIR1	125.93	99.95
			PC2_NIR1	0.04	0.04
NIR2	860–1 040	181	PC1_NIR2	176.22	97.36
			PC2_NIR2	3.39	1.87
b)					
Coastal	400–450	51	PC1_Coastal	50.27	98.58
			PC2_Coastal	0.32	0.64
Blue	450–510	61	PC1_Blue	60.47	99.14
			PC2_Blue	0.41	0.68
Green	510–580	71	PC1_Green	69.60	98.04
			PC2_Green	1.21	1.71
Yellow	585–625	41	PC1_Yellow	40.76	99.43
			PC2_Yellow	0.13	0.34
Red	630–690	61	PC1_Red	60.11	98.55
			PC2_Red	0.72	1.19
Red-edge	705–745	41	PC1_Red-edge	37.08	90.46
			PC2_Red-edge	3.86	9.42
NIR1	770–895	126	PC1_NIR1	125.87	99.90
			PC2_NIR1	0.08	0.07
NIR2	860–1 040	181	PC1_NIR2	177.08	97.84
			PC2_NIR2	2.34	1.30

PCs principal components, *NIR* near-infrared

the different weight of the spectral bands to determine the greenness and vigor of canopy as a function of the phenological stage. In particular, at anthesis, the Green band seemed to be a better indicator of plant vigor than the Red one.

The differences among the short-range factors at the two growth stages can also be detected in the Fig. 5a, b. To facilitate interpretation of the F1 maps, the variation range of the factor scores was divided into three iso-frequency classes, to represent low, medium

Table 2 Loading values of the first regionalized factors (F1), corresponding eigen-value and explained variance (%) at each spatial scale (for the two sampling dates, March and April)

	F1_March (60 m)	F1_April (80 m)
PC1_Coastal	−0.4237	0.2147
PC1_Blue	−0.4279	0.0658
PC1_Green	−0.1362	−0.5497
PC1_Yellow	−0.4055	−0.3285
PC1_Red	−0.4188	−0.2246
PC1_Red-edge	0.2459	−0.4909
PC2_Red-edge	−0.3014	0.1456
PC1_NIR1	0.2214	0.1931
PC1_NIR2	0.2804	0.4355
Eigen val.	4.1822	1.8261
Var. Perc.	94.36	95.99

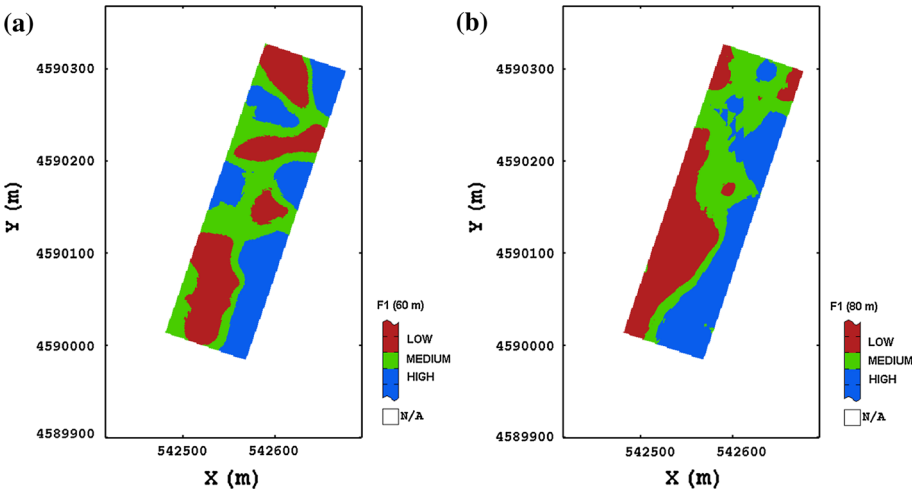

Fig. 5 Classification of the standardized regionalized factors (F1) with short range for each crop growth stage: **a** March (60 m) and **b** April (80 m), obtained by splitting the overall range of variation into three equal quantiles

and high values of plant vigor and greenness. In March the map (Fig. 5a) displayed high values along the eastern side and low values in the north and south-east zones. In April the F1 map (Fig. 5b) highlighted the western and northern parts with the lowest values, and a persistent area of higher values along the eastern side of the field.

Crop N status

N-uptake was significantly and positively correlated ($p < 0.05$) with PC1_NIR1, PC1_NIR2 and PC2_Red-edge and this result determined the choice of the multivariate data set to be submitted to the geostatistical analysis. A linear model of co-regionalization

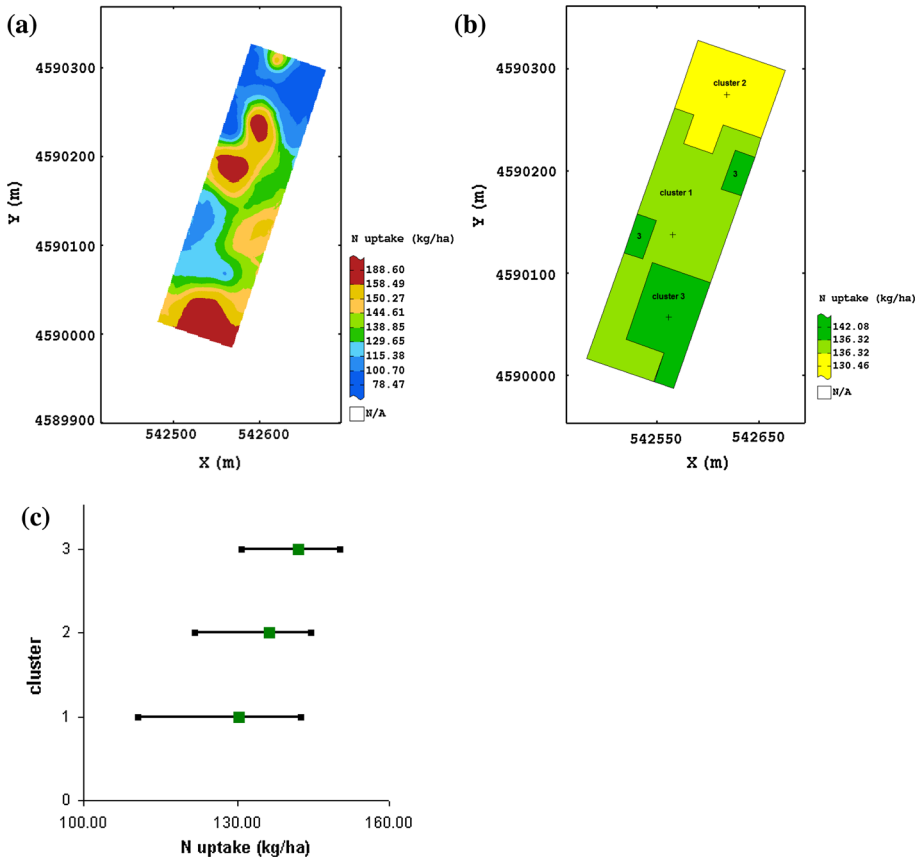

Fig. 6 Spatial map (**a**), map of the variable obtained by using polygon kriging (**b**), and 95 % lower limit, expected value, 95 % upper limit of CI for N-uptake (**c**)

was fitted including, as basic structures, a nugget effect and a spherical model with range of 51.97 m. The goodness of fitting was generally satisfactory, because the mean error and the mean squared standardized error were close to zero (−0.081) and one (0.889), respectively.

N-uptake map (Fig. 6a) showed two wide areas in the middle and south-western parts of the field characterized by higher values rather reproducing the spatial patterns of the hyperspectral factor (F1) in April (Fig. 5b). This would suggest the predictive capacity of hyperspectral data for crop N-status, in agreement with other studies (Li et al. 2010).

In order to disclose differences of the crop N-status among the clusters, the expected values of N-uptake with the corresponding CIs were compared (Fig. 6b, c). Although the clusters did not differ significantly, owing to the large within-cluster variability, cluster 2 showed the lowest expected value.

Grain yield results of two cropping seasons

To test the effectiveness of SSP organic fertilization, wheat grain yield after uniform distribution of fertilizers (2009–2010 season) was compared with the yield after SSP

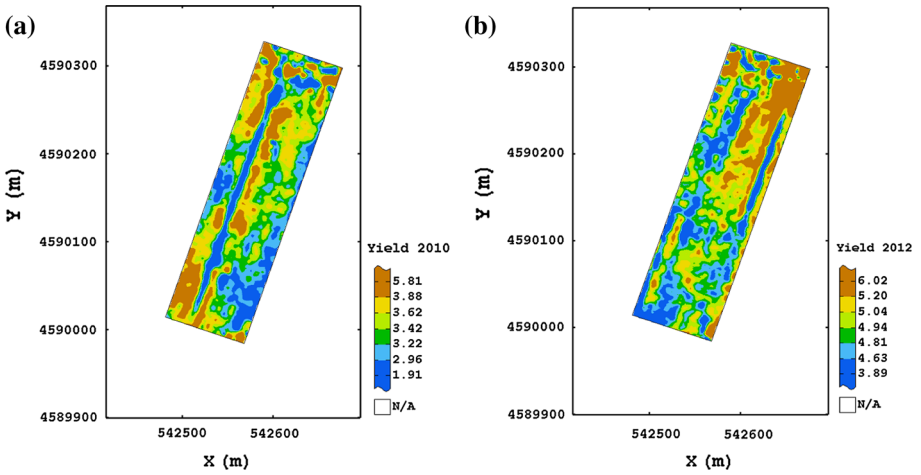

Fig. 7 Spatial maps of 2010 (**a**) and 2012 (**b**) wheat grain yield (t ha^{-1})

fertilization (2011–2012 season) (Fig. 7a, b). Despite the two yield maps looked quite noisy, they showed a northern area which was tendentially more productive than the southern area of the field. As regards the narrow strip of low yield running parallel to the longitudinal axis in the western part of the field, it was persistent in both seasons and was probably due to soil compaction, caused by the presence of a previous rural road. This compaction may have prevented root system development and water uptake, negatively affecting wheat production.

The mean yield value of 2009–2010 yield (3.41 t ha^{-1}) was higher than that (2.71 t ha^{-1}) of the later drier season of wheat cultivation. Of course, the rainfall trend influences the wheat response to N availability, thus the observed spatial patterns of wheat yield were quite likely affected by differences in available soil water distribution over the two seasons. Figure 7a, b showed that the range of yield variation was narrower in the 2011–2012 season, with the minimum and the maximum values greater than the corresponding values of the 2009–2010 season. The greater spatial yield uniformity observed in the later season might be attributed to the SSP fertilization and/or to different meteorological conditions. Moreover, to compare the productivity potential of each cluster, the expected values with their CIs are reported in Fig. 8. The cluster 2 was the most productive in both seasons though in 2010 it was not significantly different than cluster 1. Cluster 3 was significantly less productive in 2010, and in the later season it did not differ significantly than cluster 1. In any case, the within-cluster variance for yield was reduced in 2012. A difference of 12 and 5 % between the highest and lowest values was detected in the first and second season, respectively. These results might be as a consequence of climatic conditions and might be also ascribable to an effect of leveling out in the clusters due to the SSP fertilization, which is one of the targets of PA.

Relationship between crop growth response and wheat grain yield

In 2011–2012 season a general inverse relation between grain yield and crop N-status can be observed in the maps of the Figs. 7 and 5. This might be mainly due to the cumulative

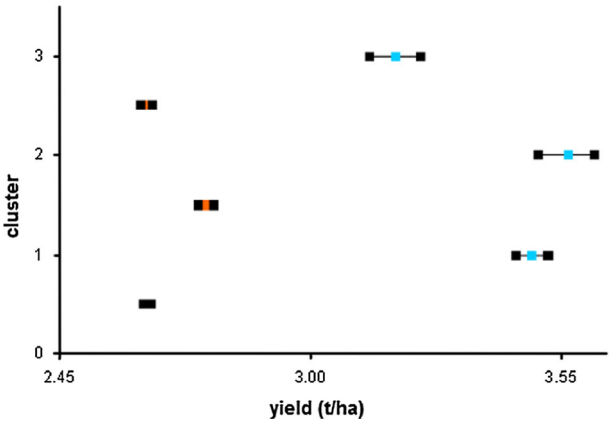

Fig. 8 95 % lower limit, expected value (*blue* and *red* for the 2010 and 2012 results, respectively), 95 % upper limit of CI for yields (Color figure online)

Table 3 Contingency tables between yield classes and N-uptake classes

clyield[a]	clN-uptake[b]			
	h	l	m	Total
h	2 767	4 818	3 271	10 856
	9.05	15.75	10.69	35.49
	25.49	44.38	30.13	
	26.58	47.73	32.44	
l	4 242	2 680	3 071	9 993
	13.87	8.76	10.04	32.67
	42.45	26.82	30.73	
	40.75	26.55	30.46	
m	3 402	2 596	3 741	9 739
	11.12	8.49	12.23	31.84
	34.93	26.66	38.41	
	32.68	25.72	37.10	
Total	10 411	10 094	10 083	30 588
	34.04	33.00	32.96	100.00
S	79.0054		Pr > S	< 0.0001
k	−0.0291			
95 % Lower	−0.0378			
95 % Upper	−0.0204			

Each cell gives the frequency, percentage of the total frequency, the row percentage and the column percentage

a, b classes for yield and N-uptake, respectively, *h* high, *m* medium, *l* low, *S* statistic by test of symmetry *k* weighted kappa coefficient, *95 % Lower and Upper k* confidence limits

Table 4 Contingency tables between yield classes and two F1 classes at the shorter scale: 60 m for March (a) and 80 m for April (b)

clyield[a]	clF1_March[b]			
	h	l	m	total
a)				
h	3 495	3 963	3 398	10 856
	11.43	12.96	11.11	35.49
	32.19	36.51	31.30	
	32.93	39.00	34.63	
l	3 880	3 014	3 099	9 993
	12.68	9.85	10.13	32.67
	38.83	30.16	31.01	
	36.55	29.66	31.58	
m	3 240	3 184	3 315	9 739
	10.59	10.41	10.84	31.84
	33.27	32.69	34.04	
	30.52	31.34	33.79	
Total	10 615	10 161	9 812	30 588
	34.70	33.22	32.08	100.00
S	5.7891		Pr > S	0.1223
k	−0.0060			
95 % Lower	−0.0148			
95 % Upper	0.0028			
b)				
h	2 553	3 624	4 679	10 856
	8.35	11.85	15.30	35.49
	23.52	33.38	43.10	
	24.41	35.80	46.77	
l	4 162	3 226	2 605	9 993
	13.61	10.55	8.52	32.67
	41.65	32.28	26.07	
	39.79	31.86	26.04	
m	3 744	3 274	2 721	9 739
	12.24	10.70	8.90	31.84
	38.44	33.62	27.94	
	35.80	32.34	27.20	
Total	10 459	10 124	10 005	30 588
S	217.0939		Pr > S	< 0.0001
k	−0.1191			
95 % Lower	−0.1276			
95 % Upper	−0.1106			

Each cell gives the frequency, percentage of the total frequency, the row percentage and the column percentage

a, b, c classes for yield, F1 of March and April, respectively, *h* high, *m* medium, *l* low, *S* statistic by test of symmetry, *k* weighted kappa coefficient, *95 % Lower and Upper k* confidence limits

rainfall in the latest growth stages (May–June), which was characterized by values lower by 197 and 269 % compared to the ones of the 2009–2010 season and the long term period, respectively. Therefore, the areas with better N-status, and consequently greater plant vigor, were more "water stressed". A too vigorous crop in the vegetative stage generally transpires too much water, which can result in low grain yield.

Table 3 shows the spatial association between yield classes and N-uptake classes. The overall agreement was 30 % and the Bowker's test of symmetry (Bowker 1948) showed that the hypothesis of homogeneity between the two maps cannot be accepted. The *k* coefficient, although significantly different from 0, showed a negative value, indicative of poor spatial agreement. Also, the CIs confirmed that the true *k* value was greater than zero. Since the medium class is a transition class, only the high and low classes are commented. More than 44 % of the high yield class occurred at the low class of N-uptake. Conversely, about 42 % of the low yield class occurred at the high class of N-uptake. The total accordance between high–high and low–low classes was only 9.05 and 8.76 %, respectively.

Table 4 a, b show the association between the yield classes and the classes of the two F1 s at short scale (60 and 80 m for March and April, respectively), assumed as indices of plant vigor.

The overall agreement was 32 and 27 % at the first and the second GS, respectively. In both cases, the Bowker's test of symmetry showed that the hypothesis of homogeneity between the two maps cannot be accepted. The *k* coefficient, although significantly different from 0, showed low absolute values, indicative of a poor spatial agreement, and the CI of *k* showed that it was significantly less than zero. The percentage of the high class of yield occurring at the low class of F1_March was 36 %, whereas the percentage of the low yield class occurring at the high class of F1_March was approximately 39 %. More than 33 % of the high yield class occurred at the low class of F1_April, and approximately 42 % of the low yield class occurred at the high class of F1_April.

On the whole, the results of the quantitative comparisons through the contingency matrices confirm the inverse relationship between grain yield and crop growth response, that was more accentuated at GS 60, previously detected from a visual inspection of the maps.

Conclusions

This study has presented a multivariate combined statistical and geostatistical approach to assess the effects of site-specific organic fertilization on wheat growth and yield, in transition to organic agriculture.

The small difference in the N rates applied to clusters came out from the specific field-trial conditions, whereas higher differences in N rates could possibly be obtained in other case studies.

The acquisition of very fine-scale information on plant, by using hyperspectral measurements, has proved to be effective in assessing spatial variability of crop response and particularly for helping to predict crop N-status at the beginning of anthesis. Data processing through PCA and FKA allowed to remove the redundant information given by neighbouring bands and synthesize the observed multivariate variation.

The changes in spatial yield pattern over the seasons highlighted the influence of meteorological conditions under rainfed cultivation. This influence is also detectable by the inverse relationship between crop N-status and grain yield after precision fertilization. It

can be suggested that a higher demand for water in areas of the field with better N-status, caused by higher transpiration surface, has reduced grain yield under water stress conditions. Also, drought stress and high temperatures during grain filling may have induced early senescence and reduced yield. If the wheat yield was mostly related to the rainfall, the difference in spatial distribution of crop response in different cropping seasons might be ascribable in part to the climatic conditions and in part to management. In our case the combined effect was a reduction of within-management zone variance for yield over time. Despite the shortness of the surveying period, these preliminary results seem to be quite positive and promising in the perspective of the PA that aims, among other things, to level the overall soil fertility and plant response.

Acknowledgments The work has been supported by Italian Ministry of Agriculture and Forestry Policies under contract no. 24324/7742/2009 ("Sistemi colturali e interventi agronomici innovativi in agricoltura biologica" BIOINNOVA, Coordinator: Dr. Domenico Ventrella, CRA—SCA, Research Unit for Cropping Systems in Dry Environments, Bari). The authors thank M. Mastrangelo for his skilful technical assistance for chemical analysis. This work was benefited from the fertilizer supplying for free from the ILSA S.p.A. (Dr. Eugenio Babini). The authors wish to thank also the John Deere Company (Dr. Matteo Antonello).

References

Barnes, E. M., Clarke, T. R., & Richards, S. E. (2000). Coincident detection of crop water stress, nitrogen status and canopy density using ground based multispectral data. In P. C. Robert, R. H. Rust, & W. E Larson (Eds.), *Proceedings of the 5th international conference on precision agriculture*. American Society of Agronomy, Madison.

Bowker, A. H. (1948). A test for symmetry in contingency tables. *Journal of the American Statistical Association, 43*, 572–574.

Castrignanò, A., Giugliarini, L., Risaliti, R., & Martinelli, N. (2000). Study of spatial relationships among some soil physico-chemical properties of a field in central Italy using multivariate geostatistics. *Geoderma, 97*, 39–60.

Chilès, J. P., & Delfiner, P. (1999). *Geostatistics: Modelling spatial uncertainty*. New York: Wiley.

Cohen, J. (1960). A coefficient of agreement for nominal scales. *Educational and Psychological Measurement, 20*, 37–46.

Diacono, M., Abd El Rahman, H., Cocozza, C., De Benedetto, D., Troccoli, A., Rubino, P., et al. (2011). Delineation of homogeneous field zones based on soil fertility indices in a durum wheat—Chickpea rotation. In J. V. Stafford (Ed.), *Precision agriculture 2011* (pp. 164–179). UK: Ampthill.

Diacono, M., Castrignanò, A., Troccoli, A., De Benedetto, D., Basso, B., & Rubino, P. (2012). Spatial and temporal variability of wheat grain yield and quality in a Mediterranean environment: A multivariate geostatistical approach. *Field Crops Research, 131*, 49–62.

Digital Globe. (2009). White Paper. The Benefits of the 8 Spectral Bands of WorldView-2. (p. 10). Retrieved from www.digitalglobe.com.

FAO. (1995). Sustainability issues in agricultural and rural development policies, Trainer's manual, vol 1.

Geovariances. (2012). Isatis® Technical Ref., 12.04 Geovariances and Ecole Des Mines De Paris: Avon Cedex, France.

Horneck, D. A., & Miller, R. O. (1998). Determination of total nitrogen in plant tissue. In Y. P. Kalra (Ed.), *Handbook of reference methods for plant analysis* (pp. 75–83). Boca Raton: CRC Press.

Kaiser, H. F. (1960). The application of electronic computers to factor analysis. *Educational and Psychological Measurement, 20*, 141–151.

Lajaunie, C., & Béhaxétéguy, J. P. (1989). Elaboration d'un programme d'ajustement semi-automatique d'un modèle de corégionalisation—Theorie, technical report N21/89/G. Paris: ENSMP.

Li, F., Miao, Y., Hennig, S. D., Gnyp, M. L., Chen, X., Jia, L., et al. (2010). Evaluating hyperspectral vegetation indices for estimating nitrogen concentration of winter wheat at different growth stages. *Precision Agriculture, 11*, 335–357.

Li, F., Miao, Y., Zhang, F., Cui, Z., Li, R., Chen, X., et al. (2009). In-season optical sensing improves nitrogen-use efficiency for winter wheat. *Soil Science Society of America Journal, 73*, 1566–1574.

Maeder, P., Fliessbach, A., Dubois, D., Gunst, L., Fried, P., & Niggli, U. (2002). Soil fertility and biodiversity in organic farming. *Science, 296*(5573), 1694–1697.

Matheron, G. (1982). Pour une analyse krigeante des données régionalisées. Rapport N-732. Centre de Géostatistiques, École des Mines de Paris, Fontainebleau.
Mueller, N. D., Gerber, J. S., Johnston, M., Ray, D. K., Ramankutty, N., & Foley, J. A. (2012). Closing yield gaps through nutrient and water management. *Nature, 490*(7419), 254–257.
Page, A. L., Miller, R. H., & Keeny, D. R. (1982). *Methods of soil analysis, Part II* (2nd ed.). Madison, WI: American Society of Agronomy.
Prasad, B., Carver, B. F., Stone, M. L., Babar, M. A., Raun, W. R., & Klatt, A. R. (2007). Potential use of spectral reflectance indices as a selection tool for grain yield in winter wheat under Great Plains conditions. *Crop Science, 47*, 1426–1440.
Ray, S. S., Singh, J. P., & Panigraphy, S. (2010). Use of hyperspectral remote sensing data for crop stress detection: Ground-based studies. International Archives of Photogrammetry, Remote Sensing and Spatial Information Science, vol. 38, Part 8. Kyoto, Japan.
SAS Institute Inc., (2012). SAS/STAT software release 9.3. Cary, NC: SAS Institute.
Shepherd, M. A., Davies, D. B., & Johnson, P. A. (1993). Minimizing nitrate losses from arable soil. *Soil Use and Management, 9*(6), 94–99.
Soil Survey Staff. (1999). *Soil taxonomy: A basic system of soil classification for making and interpreting soil surveys. Agriculture Handbook No. 436*, 2nd edn. Washington, DC: U.S. Gov. Print. Office.
Stellacci, A. M., Castrignanò, A., Diacono, M., Troccoli, A., Ciccarese, A., Armenise, E., et al. (2012). Combined approach based on principal component analysis and canonical discriminant analysis for investigating hyperspectral plant response. *Italian Journal of Agronomy, 7*, 247–253.
Stroppiana, D., Boschetti, M., Brivio, P. A., & Bocchi, S. (2009). Plant nitrogen concentration in paddy rice from field canopy hyperspectral radiometry. *Field Crops Research, 111*, 119–129.
Thenkabail, P. S., Enclona, E. A., Ashton, M. S., & Van Der Meer, B. (2004). Accuracy assessments of hyperspectral waveband performance for vegetation analysis applications. *Remote Sensing of Environment, 91*, 354–376.
Tubaña, B. S., Arnall, D. B., Holtz, S. L., Solie, J. B., Girma, K., & Raun, W. R. (2008). Effect of treating field spatial variability in winter wheat at different resolutions. *Journal of Plant Nutrition, 31*, 1975–1998.
Wackernagel, H. (2003). *Multivariate geostatistics: An introduction with applications* (3rd ed.). Berlin: Springer.
Walkley, A., & Black, I. A. (1934). An examination of the Degtjareff method for determining organic carbon in soils: Effect of variations in digestion conditions and of inorganic soil constituents. *Soil Science, 63*, 251–263.
Webster, R., & Oliver, M. (2001). *Geostatistics for environmental scientists. Statistics in practice*. Chichester: Wiley.
Zadoks, J. C., Chang, T. T., & Konzak, C. F. (1974). A decimal code for the growth stages of cereals. *Weed Research, 14*, 415–421.